

# Effect of cooling rate on the location and chemistry of glassy phases in silica-doped 3Y-TZP ceramics

L. Gremillard<sup>1</sup>, T. Epicier, J. Chevalier\*, G. Fantozzi

*GEMPPM UMR CNRS 5510, National Institute for Applied Sciences, 69621 Villeurbanne, France*

Received 26 January 2004; received in revised form 15 March 2004; accepted 23 March 2004

Available online 20 June 2004

## Abstract

The morphology and the composition of glassy phases in silica-doped 3Y-TZP ceramics are studied for two extreme conditions of cooling. On the one hand, materials quenched after sintering exhibit silica-rich glassy phases both at grain boundaries and multiple junctions, with an enrichment of yttrium and zirconium. These observations are related to equilibrium at high temperature. On the other hand, materials slowly cooled exhibit glassy phases only at multiple junctions. During specific conditions of cooling, it is thus shown that dewetting can occur, giving rise to a low temperature equilibrium without glassy phase.

© 2004 Elsevier Ltd. All rights reserved.

**Keywords:** ZrO<sub>2</sub>; TZP; Grain boundaries; Glassy phase; Equilibrium thickness; Electron microscopy; EELS

## 1. Introduction

The presence of glassy phases can have a profound effect on the properties of polycrystalline ceramics. Such glassy phases in ceramics sometimes result from silica-rich impurities but they can also be added during processing route in order to obtain specific physical or mechanical properties. For instance, the addition of glassy phases in yttria-doped zirconia ceramics is a way to increase their superplastic behavior<sup>1,2</sup> or their ageing resistance.<sup>3,4</sup>

If the effect of glassy phases on final properties is today commonly accepted, their morphology and chemical composition in silica-containing zirconia ceramics are still under discussion. Based on a continuum approach incorporating interfacial energies, Clarke<sup>5–7</sup> has claimed for the existence of a stable equilibrium thickness of these glassy phases in ceramics. Following these works, a number of

authors<sup>1–3,8</sup> observed intergranular non-crystalline films in silica-doped zirconia, with a constant thickness at grain boundaries and the presence of vitreous silica pockets at multiple junctions. However, others<sup>9–11</sup> only found amorphous pockets of a silica-rich phase at multiple junctions, but not at grain boundaries. In the case of Y-TZP compounds doped with alumina, no grain-boundary films were observed.<sup>12</sup> This apparent discrepancy may be due to the fact that the detection, by transmission electron microscopy (TEM), of thin non-crystalline films (of the order of 1 nm), is complex. A number of TEM techniques have been developed to detect directly or indirectly grain-boundary films. In the past, glass films at grain boundaries in silica-doped zirconia were observed by indirect methods, for example, contrast technique.<sup>13</sup> These techniques are susceptible to a number of experimental uncertainties,<sup>14</sup> which make them questionable for fine films observations in small grain size materials. Direct observations with high resolution TEM (HRTEM), associated with energy dispersive X-ray spectroscopy (EDS) or electron energy loss spectroscopy (EELS) are preferred today. This approach was used recently by Ikuhara et al.<sup>9,10</sup> and Gremillard et al.<sup>11</sup> who did not detect any glassy phase at grain boundaries in Y-TZP.

\* Corresponding author. Tel.: +33 4 72 43 61 25;  
fax: +33 4 72 43 85 28.

E-mail address: [jerome.chevalier@insa-lyon.fr](mailto:jerome.chevalier@insa-lyon.fr) (J. Chevalier).

<sup>1</sup> Present address: Lawrence Berkeley National Lab., Materials Science Division, Berkeley, CA 94720, USA.

A careful reading of Clarke's works<sup>5–7</sup> leads to propose an alternative origin for the differences noted in the literature. Indeed, glassy phases were always observed at low temperature and no information was given on the cooling rate after the sintering process. Clarke has argued on the presence of a glassy phase wetting the ceramic grains at high temperature,<sup>5–7</sup> but also on the possibility for glassy phase modification during cooling under specific conditions.<sup>15</sup> Thus, the cooling conditions after sintering may have a great influence on the microstructure: rapidly cooled or quenched materials are then expected to exhibit a microstructure close to the equilibrium state at high temperature, whereas slowly cooled materials will reach a lower temperature equilibrium state. This work aims at demonstrating the differences between these two extreme conditions in silica-doped 3Y-TZP ceramics; special attention will be paid on the location and chemistry of non-crystalline phases.

## 2. Results and discussion

Two batches of 3 mol% yttria-stabilised tetragonal (3Y-TZP) zirconia polycrystals containing 5 wt.% silica were processed using a slip-casting method (see Gremillard et al.<sup>4</sup> for details). After sintering at 1450 °C for 5 h, one batch was furnace-cooled at 300 °C/h (Z-S50), and the other quenched in air (Z-S50-Q). For

this latter, the cooling rate was estimated to be around 300 °C/min. TEM samples were prepared by dimpling and ion-milling. TEM observations were conducted on a JEOL 2010-F high-resolution microscope, equipped with a Gatan DigiPEELS analyser for electron energy loss spectroscopy.

All high resolution images on Z-S50 clearly show the absence of any glass film at grain boundaries; more than 50 general grain-boundaries were observed edge-on in HRTEM conditions (e.g., lattice fringes resolved in both adjacent grains). A selection of six pictures is shown in Fig. 1.

Consistently, nano-probe EDS (not shown here) and EELS analysis failed to detect the presence of silicium at any grain-boundary, as shown in Fig. 2 (top line). Besides it is shown that the glassy phase occasionally observed at triple junctions (last micrograph in Fig. 1) is mainly constituted of silica (Fig. 2, bottom line); no significant quantities of zirconium (and yttrium) could be detected during EELS analysis with a nanometric or sub-nanometric probe.

On another hand, a significant yttrium segregation towards most of the grain boundaries (see, for example, Fig. 3) is evidenced, in agreement with previous results.<sup>9</sup>

The microstructure of Z-S50-Q quenched materials appears to be more complex. First, a lot of grain boundaries remain glass-free (Fig. 4), whereas a significant amount (about 10 on 50 interfaces analysed in HRTEM conditions)

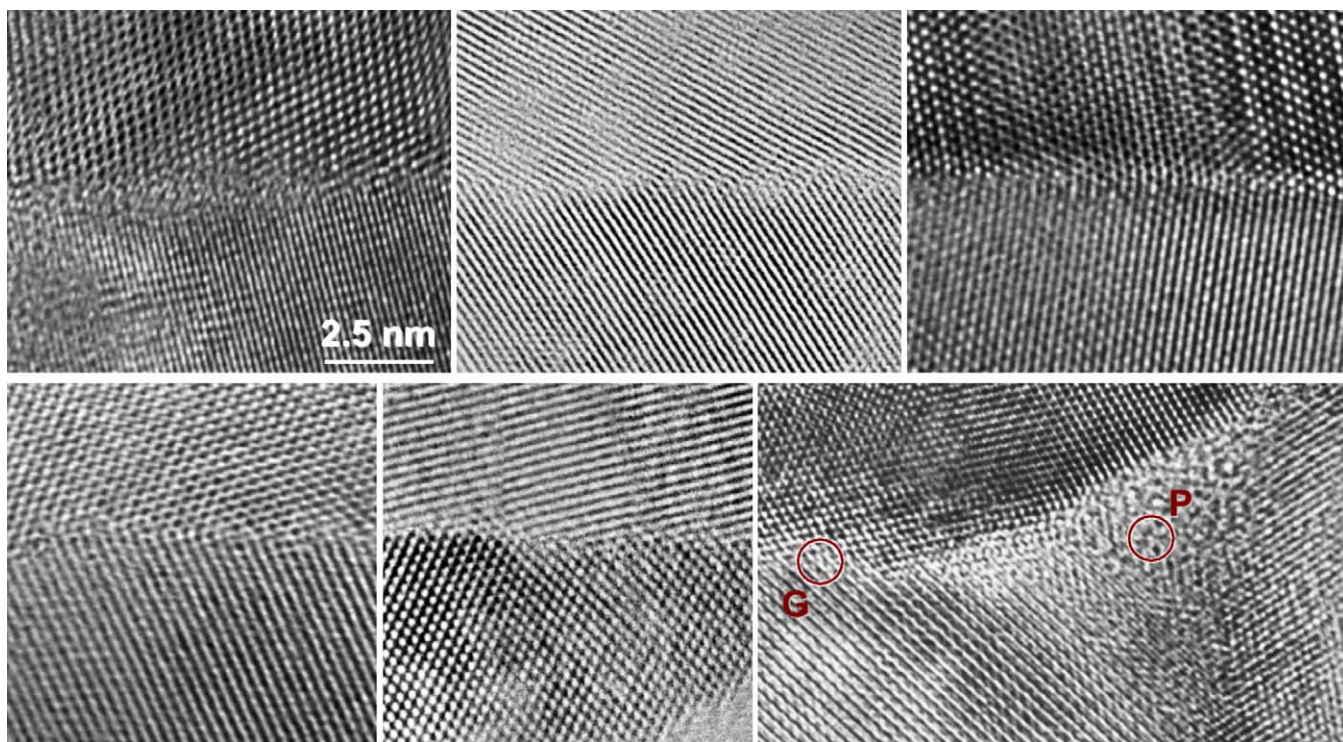


Fig. 1. HRTEM images of edge-on grain boundaries in Z-S50. The last micrograph shows a glassy pocket at a multiple junction, and G and P circles correspond to the 1 nm probe positions for the EELS analysis of the grain boundary and glassy phase, respectively (see Fig. 2).

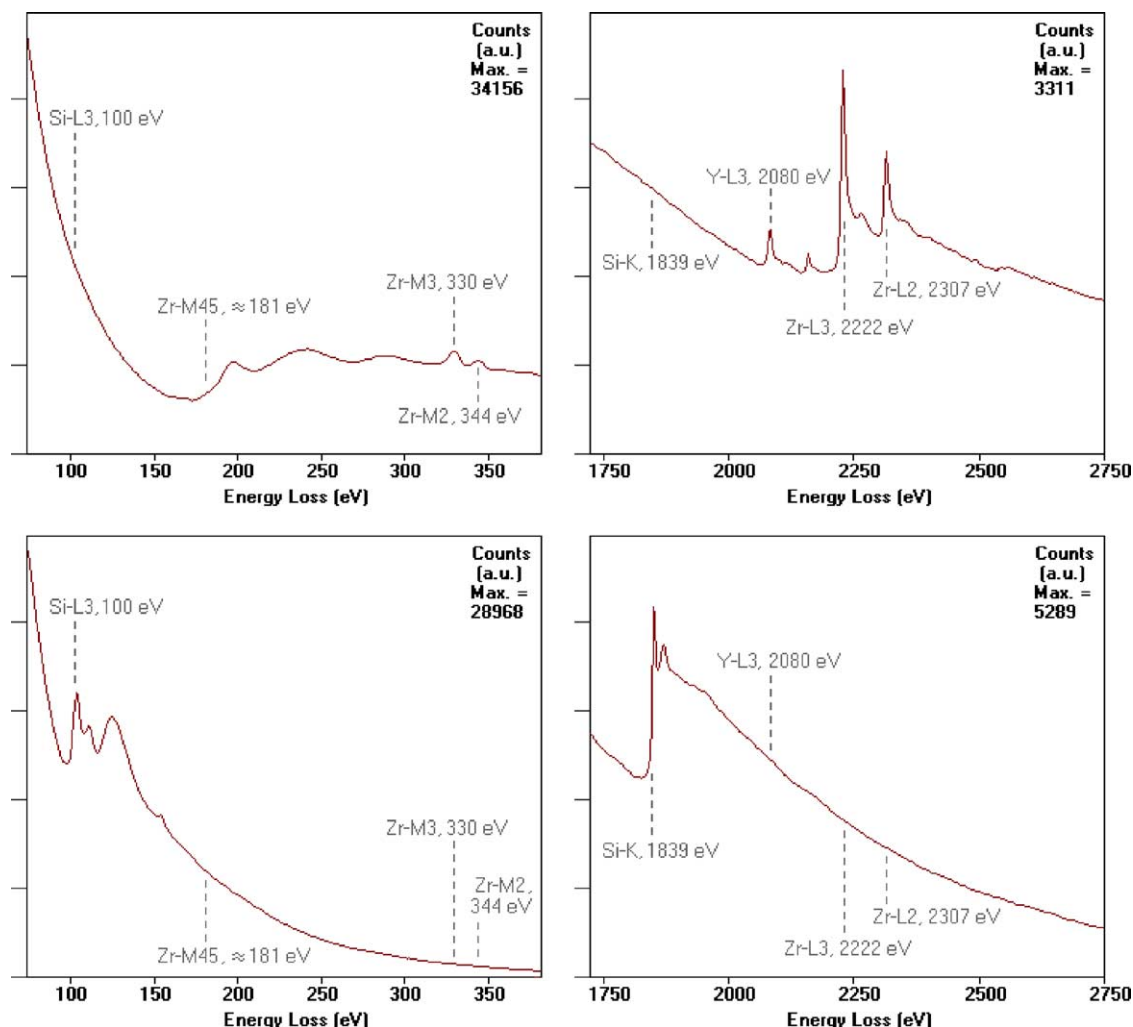


Fig. 2. EELS nanoprobes analysis of the grain-boundary and the glassy pocket in Z-S50 from Fig. 1 (top and bottom, respectively) over energy ranges including the Si-L<sub>2,3</sub> and Zr-M, and Si-K and Zr-L edges (left and right, respectively).

exhibit a glassy layer (e.g. Fig. 5). Their thickness is of about 1.8 nm, i.e. close to the equilibrium thickness calculated by Clarke.<sup>5</sup> EELS analysis (right-hand side of Fig. 5) confirms that this non-crystalline films are silica-rich. Moreover, these non-crystalline phases are unstable: during a prolonged exposure to the electron beam, a crystallisation is observed (the irradiation acting most probably as an annealing treatment) as shown by Fig. 6.

Fig. 6a shows a glassy pocket prior to irradiation; note that EELS analysis (Fig. 6b) indicate that it is not pure silica, but does contain a significant amount of zirconium and yttrium compared to the case of slowly cooled Z-S50 materials (Fig. 2). After a short irradiation time (Fig. 6c), the apparition of a 'network' is evidenced at a relatively low magnification. At higher magnification (Fig. 6d), it becomes clear that this network consists of frequently interconnected nano-crystallites (~2–10 nm in size) embedded in the glassy phase. Fourier transforms of the HRTEM mi-

crographs point out that the crystalline phase is fully consistent with zirconia (Fig. 6e), although the exact structural form (cubic, tetragonal or monoclinic) could not be ascertained accurately. Nanoprobe chemical analyses confirm this result: EELS spectra show a strong Zr enrichment within all crystallites (e.g. Fig. 6f), associated with a depletion within the surrounded glassy phase compared to the initial analysis in Fig. 6b).

In addition, another irradiation effect is observed at grain-boundary non-crystalline films, which are gradually 'thinned' during the observation, giving rise to an epitaxial crystallisation of the yttrium and zirconium contained in the glassy phase on the surrounding grains (Fig. 7). This phenomenon appears to be reproducible and can be explained in the following way: at high temperature, yttrium and zirconium progressively dissolve in a silica-rich glassy phase at grain boundaries with a probable Y/Zr ratio higher than within the zirconia grains. Electron irradiation

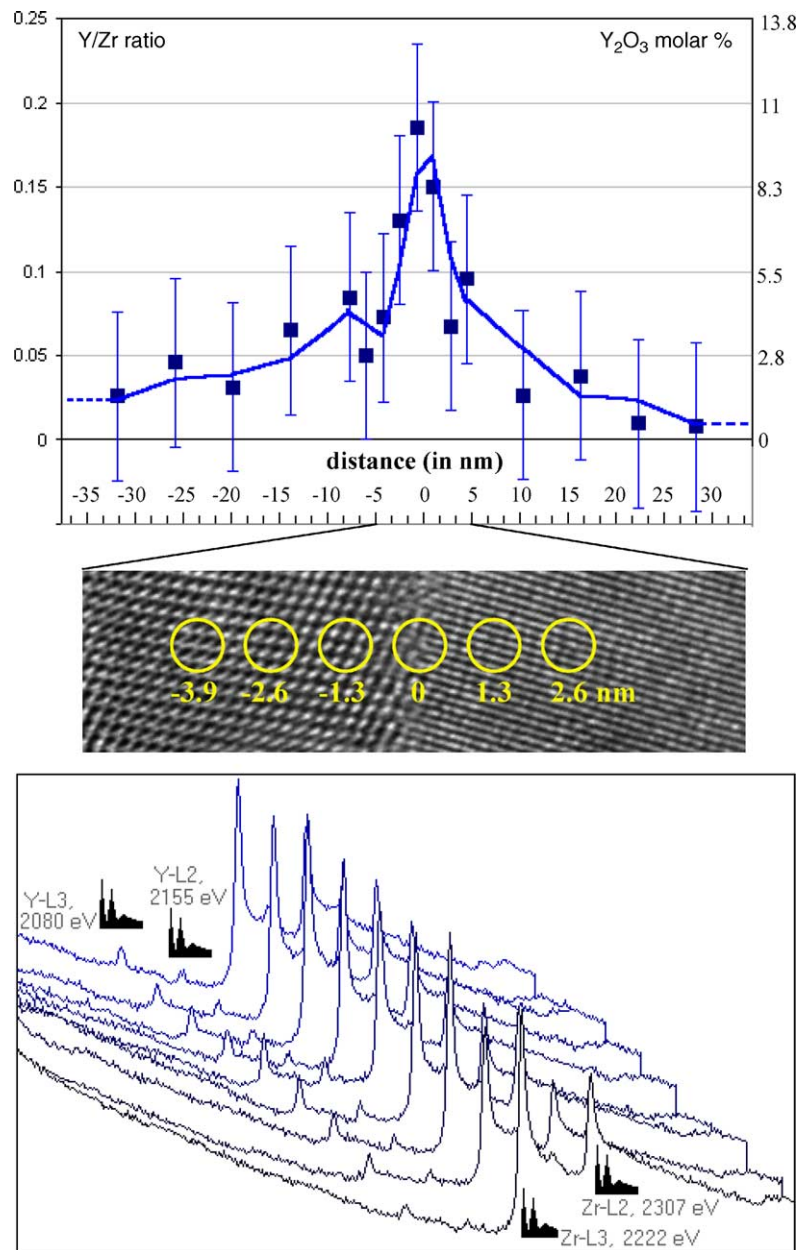


Fig. 3. EDS (top) and EELS (bottom) 1.5 nm nanoprobe line-scan of a grain-boundary in Z-S50 showing Yttrium enrichment at the interface.

tion may produce enough energy to locally activate atomic re-arrangement simulating thermal annealing. During exposure to the electron beam, phase separation thus occurs and an yttria-rich zirconia layer reprecipitates on the grain surfaces adjacent to the grain-boundaries. This interpretation

can also easily account for the yttrium enrichment at grain boundaries in Z-S50: in slowly cooled materials, the same segregation of yttria occurs because the solubility limit of Zr and Y within the glassy phase must decrease with temperature.

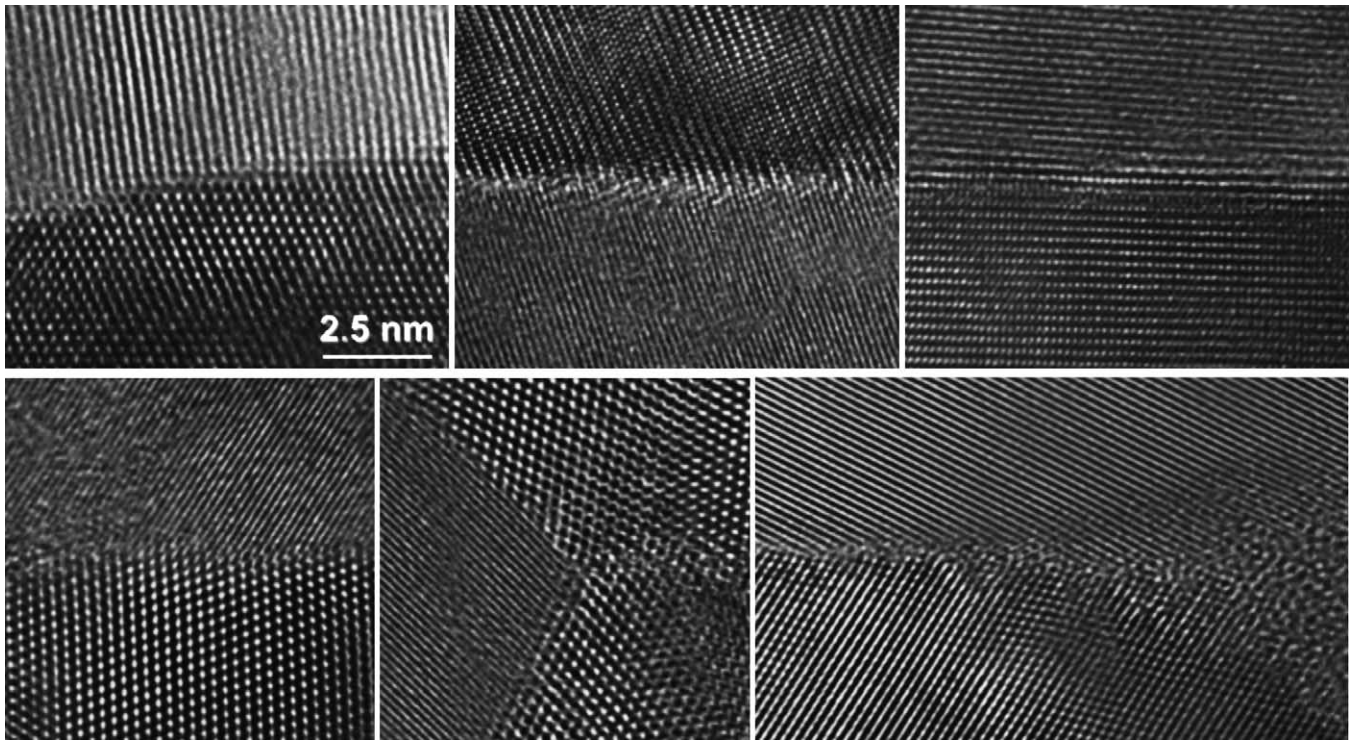


Fig. 4. HRTEM images of edge-on grain boundaries in quenched Z-S50-Q. The two last micrographs show multiple junctions without and with glassy pocket, respectively (note that the right-hand side grain boundary near the glass-free triple point correspond to a twin relation between upper and lower grains).

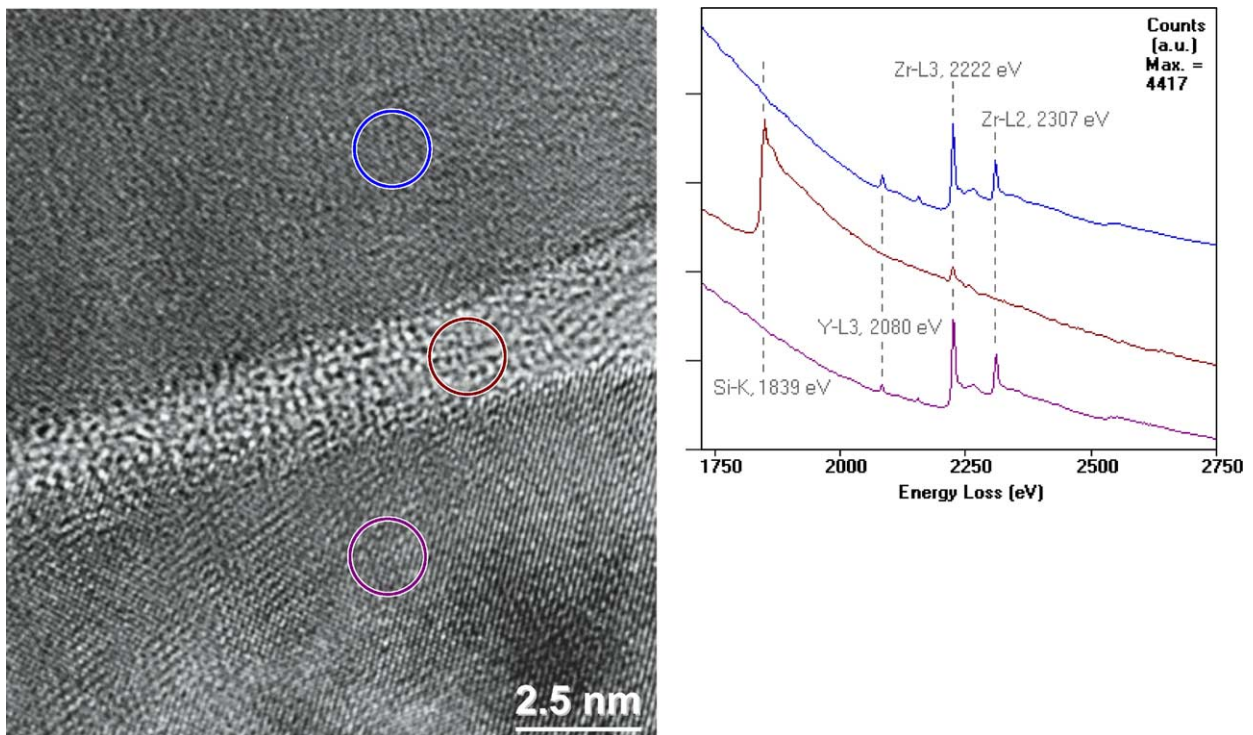


Fig. 5. Typical glassy film at a grain boundary in Z-S50-Q. Circles on the micrograph indicates the 1.5 nm probe positions at which EELS spectra have been recorded from the upper grain, the non-crystalline layer and lower grain (from top to bottom, respectively).

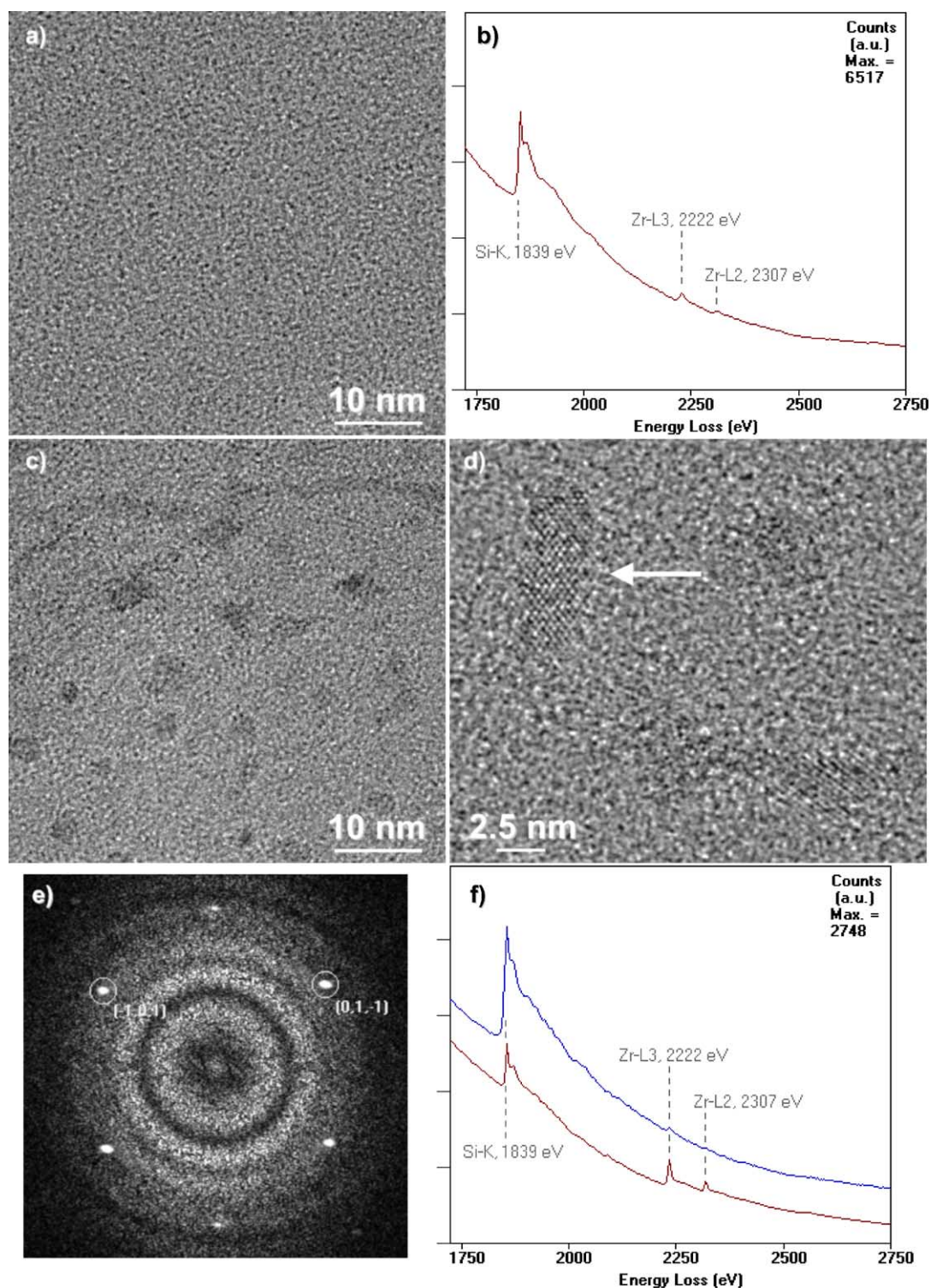


Fig. 6. Evolution of a non-crystalline pocket at a triple junction in Z-S50-Q during electron irradiation in the TEM. (a) Low-magnification HRTEM image at the beginning of observation; (b) EELS analysis corresponding to (a) (note the detection of Zr—to be compared to Fig. 2 for the slowly-cooled material); (c) same as (a) after 2 min showing the development of a crystallized 'nano-network'; (d) enlargement showing nano-crystals (e.g. arrow); (e) numerical diffractogram from particle arrowed in (d) showing lattice reflections compatible with the [111] tetragonal zirconia azimuth; (f) EELS nanoprobe analysis of the same particle (bottom spectrum) compared to that of the glassy phase (top spectrum).

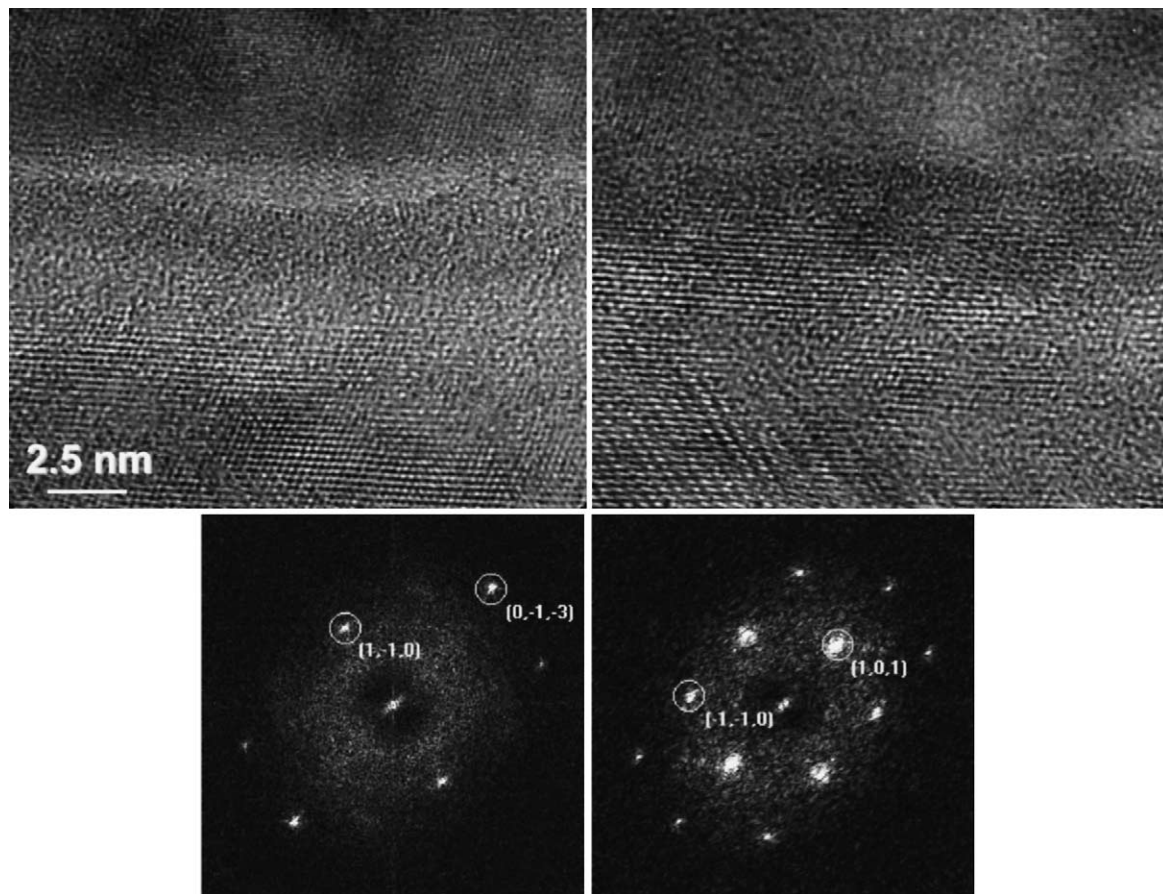


Fig. 7. Evolution of glassy film at a grain boundary in Z-S50-Q during electron irradiation in the TEM. Left: prior the observation; right: after a few minutes under the electron beam; note that the glassy boundary has been filled by a crystal with the same orientation as the inferior grain. Numerical diffractograms (bottom line) corresponding to upper and lower grains, respectively, are indexed in the  $\text{ZrO}_2$  most probable tetragonal phase ( $[-3\ 3\ 1]$  and  $[1\ -1\ -1]$  azimuths).

### 3. Conclusion

The cooling rate applied to silica-doped zirconia ceramics after sintering plays an important role on their final microstructure. When the cooling rate is high, observations are related to the high temperature equilibrium. In this case, glassy films can be present at grain boundaries and the glassy phase contains yttrium and zirconium. These films are unstable at low temperature, since they tend to crystallise under electron irradiation. When the cooling rate is low, a low-temperature equilibrium is reached and the glassy phase is only located at multiple junctions. It mainly consists of silica. Under these conditions, phase partitioning occurs during cooling, accounting for yttria segregation at grain boundaries. These observations can explain the differences noted in the literature.

### References

1. Kajihara, K., Yishizawa, Y. and Sakuma, T., The enhancement of superplastic flow in tetragonal zirconia polycrystals with  $\text{SiO}_2$  doping. *Acta Metall. Mater.* 1995, **43**, 1235–1242.
2. Hiraga, K., Yasuda, H. Y. and Sakka, Y., The tensile creep behavior of superplastic tetragonal zirconia doped with small amounts of  $\text{SiO}_2$ . *Mater. Sci. Eng. A* 1997, **234–236**, 1026–1029.
3. Mecartney, M. L., Influence of an amorphous second phase on the properties of yttria-stabilized tetragonal zirconia polycrystals (Y-TZP). *J. Am. Ceram. Soc.* 1987, **70**, 54–58.
4. Gremillard, L., Chevalier, J., Epicier, T. and Fantozzi, G., Improving the durability of a biomedical grade zirconia ceramic by the addition of silica. *J. Am. Ceram. Soc.* 2002, **85**(2), 401–407.
5. Clarke, D. R., On the equilibrium thickness of intergranular glass phases in ceramic materials. *J. Am. Ceram. Soc.* 1987, **70**, 15–22.
6. Clarke, D. R., Grain boundaries in polycrystalline ceramics. *Ann. Rev. Mater. Sci.* 1987, **17**, 57–74.
7. Bobeth, M., Clarke, D. R. and Pompe, W., A diffuse interface description of intergranular films in polycrystalline ceramics. *J. Am. Ceram. Soc.* 1999, **82**, 1537–1546.
8. Lin, Y. J., Angelini, P. and Mecartney, M. L., Microstructural and chemical influences of silicate grain boundary phases in yttria-stabilized zirconia. *J. Am. Ceram. Soc.* 1990, **73**, 2728–2735.
9. Ikuhara, Y., Thavorniti, P. and Sakuma, T., Solute segregation at grain boundaries in superplastic  $\text{SiO}_2$ -doped TZP. *Acta Mater.* 1997, **45**, 5275–5284.
10. Ikuhara, Y., Yamamoto, T. and Kuwabara, A., Structure and chemistry of grain boundaries in  $\text{SiO}_2$ -doped TZP. *Sci. Tec. Adv. Mater.* 2001, **2**, 411–424.

11. Gremillard, L., Epicier, T., Chevalier, J. and Fantozzi, G., Microstructural study of silica-doped zirconia ceramics. *Acta Mater.* 2000, **48**, 4647–4652.
12. Ross, I. M., Rainforth, W. M., Mc Comb, D. W., Scott, A. J. and Brydson, R., The role of trace additions of alumina to yttria-tetragonal zirconia polycrystals (Y-TZP). *Scripta Mater.* 2001, **45**, 653–660.
13. Clarke, D. R., On the detection of thin intergranular films by electron microscopy. *Ultramicroscopy* 1979, **4**(1), 33–44.
14. Cinibulk, M. K., Kleebe, H. J. and Rühle, M., Quantitative comparison of TEM techniques for determining amorphous intergranular film thickness. *J. Am. Ceram. Soc.* 1993, **76**, 426–432.
15. Clarke, D., High-temperature microstructure of a Hot Pressed Silicon Nitride. *J. Am. Ceram. Soc.* 1989, **72**, 1604–1609.